^{51}V NMR studies of transferred hyperfine effects in the rare-earth vanadates

Monisha Bose, Sanjukta Ganguli, and Manoranjan Bhattacharya
Saha Institute of Nuclear Physics, Calcutta 9, India
(Received 24 May 1978)

^{51}V ($I = 7/2$) NMR investigation in the whole set of rare-earth vanadates (RVO_4) in the polycrystalline form at 300 K has revealed transferred hyperfine effects. It has been observed that the ^{51}V NMR line shape strongly depends on the relative strength of the magnetic and quadrupolar parts of the transferred hyperfine interaction. On the basis of the powder pattern the RVO_4 system may be divided into two halves. The first-half members always exhibit a quadrupolar split central transition in the frequency range 2–12 MHz, whereas the members of the second half exhibit at higher frequencies an asymmetric line which, however, splits as the frequency is lowered. The hyperfine-interaction parameters, viz., the isotropic shift K_{iso}, the anisotropic shift K_{an}, and the quadrupolar coupling constant e^2qQ/h have been estimated from the central transition. The linear plot of K_{iso} against calculated $\langle S_z \rangle$ values of rare-earth ions is indicative of the contact nature of K_{iso}. Though K_{an} is dominated by the dipolar part, a small amount of anisotropic hyperfine part K_{an}^{hf} could be separated from the experimental shift. Thus the results of both K_{iso} and K_{an}^{hf} seem to uphold the presence of a small amount of covalent contribution ($f_s \sim 0.01\%$ and $f_p \sim 0.0001\%$) in these basically ionic compounds. A comparison of the ligand NMR shifts in $3d$ and $4f$ systems (oxysalts) suggests that the mechanism of spin transfer within the oxyanion is not the same in these two series. Finally, the e^2qQ/h values (0.400–0.300 MHz) exhibit a gradual decrease along the isostructural series of RVO_4. The value of the coupling constant and its variation across the rare-earth series in different compounds have been qualitatively interpreted by taking into account the bonding effects.

I. INTRODUCTION

In recent times there has been a great deal of experimental and theoretical interest[1-3] in the RXO_4 system, where R is a trivalent rare-earth ion and X is P, V, or As. Of these, the rare-earth vanadates, particularly of Tb, Dy, and Tm, have provided a set of ideal transparent cooperative Jahn Teller (CJT) compounds, and different aspects of their behavior, including magnetic ordering, have been investigated. Though $GdVO_4$ does not show CJT effect down to 0.5 K, the mixed crystal[4] $Tb_cGd_{1-c}VO_4$ is a CJT system. Apart from the CJT and low-temperature magnetic-ordering transitions, the anisotropic magnetic properties in the undistorted high-temperature tetragonal phase of the vanadates of Nd, Tb, Dy, and Tm have been studied.[5] Results of magnetic-field-induced changes in the elastic-wave propagation in these vanadates are compared to predictions of a theory based on finite deformation (considering the paramagnetic ions as pseudospins). Magnetic systems with singlet ground state at low temperature showing Van Vleck paramagnetism have also attracted attention.[6] The field-induced large electronic magnetic moment through the strong magnetic hyperfine interaction produces a nuclear Zeeman interaction of an order of magnitude greater than the true Zeeman interaction. Enhanced nuclear magnetism in the case of ^{165}Ho in $HoVO_4$ and ^{141}Pr in $PrVO_4$ has actually been observed[7,8] very recently.

The RXO_4 compounds are predominantly ionic, but possibly with a small admixture of covalency. NMR study of transferred hyperfine effects in these compounds would throw light on the bonding situation, which, in turn, is related to the chemical and magnetic properties. However, NMR of rare-earth nuclei (if not in the singlet ground state) is not observable. As such, the hyperfine interaction in the RXO_4 system has to be studied from ligand NMR effects. This has been done in the case of RPO_4 from ^{31}P ($I = \frac{1}{2}$) NMR studies[9] and information on the nature of magnetic hyperfine interaction has been obtained. The present paper is concerned with ^{51}V ($I = \frac{7}{2}$) transferred hyperfine studies[10,11] of the whole set of rare-earth vanadates, wherein magnetic interaction arising from the $4f$ rare-earth spin is interwoven with quadrupolar-interaction effects. The variation of the magnetic interaction across the series and the effect of the slowly varying lattice parameters on the quadrupolar coupling constant is revealed. Although data on the transferred hyperfine effect on the ligand nuclei directly attached to R^{3+} are available,[12-16] work on the next-nearest-neighbor (NNN) ligand nuclei is really meager.[17] NMR study of X nuclei in the oxysalts like RXO_4 would reveal the transferred hyperfine effect across the intervening oxygen atom on the second-nearest neighbor.

II. TRANSFERRED HYPERFINE EFFECTS

In predominantly ionic paramagnetic complexes, the ligand hyperfine interaction with the magnetic ion is in essence the interaction of the net electron

spin on the ligand atom with its nuclear spin.

The Hamiltonian for the ligand nucleus having spin $I > \frac{1}{2}$ in a magnetic field H_0 becomes

$$\mathcal{H} = \mathcal{H}_0 + \mathcal{H}_M + \mathcal{H}_Q \ . \tag{1}$$

Here, $\mathcal{H}_0 = -\gamma\hbar I_z H_0$ is the Zeeman term and $\mathcal{H}_M = \vec{I} \cdot \vec{A}^j \cdot \langle \vec{S}^j \rangle$ presents the magnetic hyperfine interaction between the nuclear spin I and the electron spin S, respectively; $\vec{A}^j$ is the coupling tensor of the nucleus with the jth magnetic neighbor. Lastly,

$$\mathcal{H}_Q = [e^2qQ/4I(2I-1)][3I_z^2 - I^2 + \eta(I_+^2 + I_-^2)]$$

gives the electrostatic hyperfine interaction between the electric quadrupole moment eQ of the nucleus and eq, the gradient of the electric field produced by the electronic charges both on the atom in question and on the neighbors.

In the high-field case, the sum $\mathcal{H}_M + \mathcal{H}_Q \ll \mathcal{H}_0$ and is treated as the perturbation on $\mathcal{H}_0$. Where the only perturbation on $\mathcal{H}_0$ is $\mathcal{H}_M$, the hyperfine coupling tensor $\vec{A}^j$ of $\mathcal{H}_M$ can be split up into a scalar A_s and a traceless tensor A_p. Further, if one assumes the equivalence of all the bonds and the axial symmetry of the hyperfine tensor, $\mathcal{H}_M$ takes the form[18-20]

$$\mathcal{H}_M = N'[A_s + A_p(3\cos^2\theta - 1)] I_z \langle S_z \rangle \ . \tag{2}$$

Here N' represents the number of nearest magnetic neighbors. From Eqs. (1) and (2) it is evident that the experimental resonance frequency is

$$\nu_{m \leftrightarrow m-1} = \nu_R(1 + K). \tag{3}$$

The total fractional resonance shift K may be written as the sum of isotropic shift $K_{\rm iso}$ and anisotropic shift $K_{\rm an}$ given by

$$K = K_{\rm iso} + K_{\rm an}(3\cos^2\theta - 1). \tag{4}$$

Further, if in the other limit $\mathcal{H}_m \sim 0$, $\mathcal{H}_Q$ is the only perturbing term that splits the magnetic resonance line into $2I$ components. The $m \longleftrightarrow m-1$ transition frequencies obtained from second-order perturbation treatment[21] are given by

$$\nu_{m \leftrightarrow m-1} = \nu_R + \tfrac{1}{2}\nu_Q(3\mu^2 - 1)(m - \tfrac{1}{2}) + \frac{\nu_Q^2}{32\nu_R}(1-\mu^2)\{[102m(m-1) - 18I(I+1) + 39]\mu^2 - [6m(m-1) - 2I(I+1) + 3]\}, \tag{5}$$

where

$$\mu = \cos\theta \quad \text{and} \quad \nu_Q \equiv 3e^2qQ/2I(2I-1)h \ .$$

When both $\mathcal{H}_M$ and $\mathcal{H}_Q$ are present, and if it is assumed that the principal axes of the electric-field-gradient tensor and the magnetic-shift tensor are coincident, the resonance condition is obtained from Eqs. (3)–(5), and is given by

$$\nu_{m \leftrightarrow m-1} = \nu_0 + \tfrac{1}{2}\nu_Q(3\mu^2 - 1)(m - \tfrac{1}{2}) + (\nu_Q^2/32\nu_0)(1-\mu^2)\{[102m(m-1) - 18I(I+1) + 39]\mu^2 - [6m(m-1) - 2I(I+1) + 3]\} + a(3\mu^2 - 1), \tag{6}$$

where

$$\nu_0 = \nu_R(1 + K_{\rm iso}) \quad \text{and} \quad a = K_{\rm an}/(1 + K_{\rm iso}) \ .$$

In a paramagnetic specimen one has to consider shifts resulting from the local field. This local field produces an isotropic shift and anisotropic broadening in powders. Thus when dealing with experimental shift, one has to estimate the local-field contribution[12,22,23] to obtain the shifts due to hyperfine effects alone. Further, the electric field at the nuclear site may arise from the following two sources.[24] The formation of metal-ligand covalent bond is due to transfer of electrons from the ligand valence shell to metal orbitals. This charge transfer from the ligand valence shell gives rise to quadrupolar interaction. In addition to this contribution from the valence electrons, there is also a contribution (to the field gradient) arising from all the point charges surrounding the nucleus. This contribution is a characteristic of the lattice symmetry. The experimental value of the field gradient is thus composed of contributions arising from the above two sources.

III. EXPERIMENTAL

Rare-earth vanadates melt at very high temperatures. As such, it is not very easy to produce single crystals large enough for NMR work. Therefore, the work reported here is on polycrystalline samples. The usefulness of investigations in powders in the absence of good single crystals has been discussed elsewhere.[25] Rare-earth vanadates have been prepared in the polycrystalline form following the method of Schwartz.[26] The crystal structure[27] of $LaVO_4$ prepared in this method is

monoclinic, while the structure for the rest of the vanadates is tetragonal with space group $C_{2h}^5(P_{2_1/n})$ and $D_{4h}^{19}(I4/amd)$, respectively.

Varian's variable frequency (2–16 MHz) V-4200B wide line spectrometer and a V-2100B magnet power supply unit are used for all NMR measurements. Shifts are measured with respect to ^{51}V resonance in NH_4VO_3 solution.

In the present work, 300 Oe or more is scanned and a calibration over the entire region is needed, taking into account the nonlinearity of the large scanning field. This has been done by observing the resonance of a number of nuclei, viz., ^{23}Na, ^{27}Al, ^{89}Br, and ^{13}C, as the resonance frequency of these nuclei are close to that of ^{51}V at a fixed Zeeman field. Before recording the spectrum a portion of the dial attached to the scanning unit is selected such that it corresponds to a known region of the magnetic field to be scanned. The cycling of this portion of the dial for a few times ensures the magnetic field to track a single hysteresis loop. This procedure keeps the reference signal always at the same position for the entire duration of the work.

The signal-to-noise ratio of ^{51}V NMR in RVO_4 was not very satisfactory with polycrystalline samples. To overcome this difficulty, pressed pellets have been used. Spectra in powdered and pellet form are almost identical, as in the case of the RPO_4 system.[9]

IV. RESULTS

This paper will present the results of ^{51}V NMR of 13 members in the RVO_4 series, where all the $2I$ transitions (central and all satellites) have been detected for paramagnetic members. It may be pointed out that in addition to our work,[10,11] only

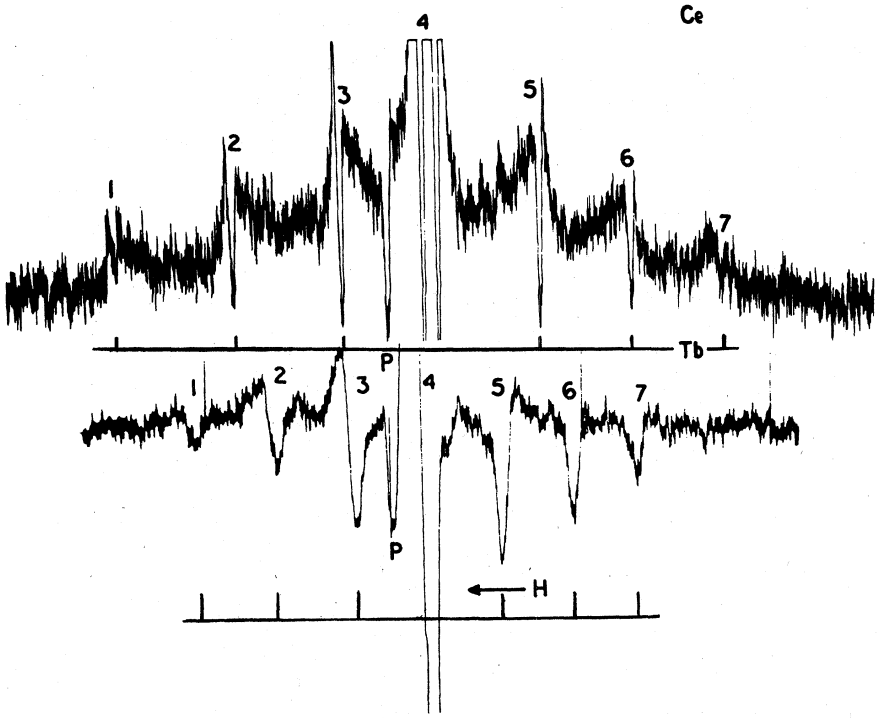

FIG. 1. ^{51}V NMR powder pattern (dispersion derivative) in $CeVO_4$ and $TbVO_4$ at 12 MHz. Transitions $m \leftrightarrow m-1$ are labeled by positive integers: 1 ($m=\frac{7}{2}$); 2 ($m=\frac{5}{2}$); 3 ($m=\frac{3}{2}$); 4 ($m=\frac{1}{2}$); 5 ($m=-\frac{1}{2}$); 6 ($m=-\frac{3}{2}$); 7 ($m=-\frac{5}{2}$). The signal of ^{27}Al from the probe material is indicated by P. The increasing direction of the magnetic field H is shown by an arrow. The field scale being slightly nonlinear is not shown. However, the field values (kOe) at the satellite peak positions are given as follows:

	Transitions labeled by					
	1	2	3	5	6	7
Ce	11.281	11.070	10.909	10.551	10.413	10.248
Tb	11.162	11.027	10.888	10.586	10.448	10.319

two incomplete NMR work[28,29] on this series have been reported so far in the literature. Saji *et al.*[28] failed to detect the ^{51}V NMR except the central component of $NdVO_4$. Pletnev *et al.*[29] reported NMR results on the whole series of vanadates. However, they also could not observe all the satellites, particularly for the second-half members. Their results on e^2qQ are more or less in agreement with ours, whereas the results on the magnetic shifts are quite different. It is to be noted that they followed a different method[30] of analysis for the powder pattern. The complete spectra of a typical member of the first- and the second-half rare earths are presented in Fig. 1. Though we have investigated both the central and satellite transitions, the results of the central transition will be presented here for the sake of brevity.

A. Analysis

In the ^{51}V NMR in the RVO_4 system, the electric quadrupole interaction is present in combination with the anisotropic magnetic-shift effects. In the RVO_4 system, considering the geometry of the VO_4 tetrahedra, one may reasonably expect an axial field gradient at the vanadium site. Moreover, the experimental ^{51}V line shape (as a function of resonance frequency) does not correspond to the case of asymmetric field gradient.[30] Thus the method of Jones *et al.*[21] which has been satisfactorily applied to a number of cases[31,32] to estimate the relevant interaction parameters, has been followed here.

Jones *et al.* have proposed that the line shape of the central transition is determined by the relative strength of the magnetic and quadrupolar interaction at a particular resonance frequency and predicted that it changes smoothly from that characteristic of quadrupolar effect to that characteristic of anisotropic-shift effect as the magnetic field strength is increased. The magnetic-shift parameters and the quadrupolar coupling constant could be obtained by measuring the shifts of the characteristic points (two singularities ν_H and ν_L and a step ν_S) of the split central transition, as given by[21]

$$\nu_H = \nu(\mu = 0) = \nu_0 + b/\nu_0 - a\nu_0, \tag{7}$$

$$\nu_L = \nu(\mu = \mu') = \nu_0 - 16b/9\nu_0 + \tfrac{2}{3}a\nu_0 - a^2\nu_0^3/4b, \tag{8}$$

$$\nu_s = \nu(\mu = 1) = \nu_0 + 2a\nu_0. \tag{9}$$

Here, $a = K_{an}/(1 + K_{iso})$ and $b = \frac{1}{16}\nu_Q^2[I(I+1) - \frac{3}{4}]$. The behavior of the singularities (ν_H and ν_L) and of the step (ν_S) in Eqs. (7)–(9) as a function of resonance frequency depends on the sign of K_{an} as well as on the relative magnitudes of K_{an} and ν_Q^2/ν_0 as shown in Fig. 2. The relative strength is represented by $r = (a/b)\nu_0^2$. ν_H and ν_L may be easily located (but not ν_S). Then Eqs. (7) and (8) may be combined in a number of ways to obtain the parameters. In the present case the expressions

$$K_H = (\nu_H - \nu_R)/\nu_R = K_{iso} - a + b/\nu_R^2 , \tag{10}$$

$$K_L = (\nu_R - \nu_L)/\nu_R = -\ (K_{iso} + \tfrac{2}{3}a) + 16b/9\nu_R^2 + a\nu_R^2/4b \tag{11}$$

have been utilized. The third term in K_L in Eq. (11) is small and may be neglected. A plot of K_H and K_L vs ν_R^2 will then yield the individual values of the parameters K_{iso}, K_{an}, and ν_Q.

The actual procedure followed for the analysis of the ^{51}V powder pattern is illustrated in Fig. 3. The line shape of the recorded spectrum (absorption derivatives) in $PrVO_4$ compares very well with the derivative of a calculated absorption line shape of Jones *et al.* with $r = \frac{25}{64}$. For shift measurement it is important to locate the actual position in the derivative of a powder spectrum, because the broadening effect shifts the peak of the absorption pattern from the point of singularity. The actual positions of ν_H and ν_L are shown by arrows on the experimental spectra. Figure 3 again shows ^{51}V pattern for $TbVO_4$, a member of the second half at 12 MHz. It has to be noted that at 12 MHz the line shape approaches the shape characteristic of an axially symmetric magnetic interaction. The structure on the low-field side indicates that K_{an} is positive. However, at lower resonance frequencies, the line is split, and thus it enabled us to measure the separate shifts of the positions ν_H and ν_L, similar to the case of $PrVO_4$.

B. Powder pattern as a function of resonance frequency

It is clear that the value of r increases with the Zeeman frequency and it is also proportional to K_{an}, which is determined by the unpaired electron magnetic moment of the rare-earth ion, the bonding situation, and crystal structure. From the similarities in the chemical properties of the rare-earth compounds in general, and also from the isostructural character of RVO_4 system (R = La–Yb), it may be expected that the bonding situation, which in turn influences the quadrupolar effect, will not show a drastic variation across the series. On the contrary, as the number of f electrons changes, the magnetic-shift interaction K_{an}, which depends on the magnetic moment, should change significantly across the rare-earth series. This change will be reflected in the r values, provided the frequency remains fixed, and will be responsible for the change in line shape across the rare-earth series. Moreover, the magnetic-shift interaction being frequency dependent, the line shape for a particular rare earth is expected to change

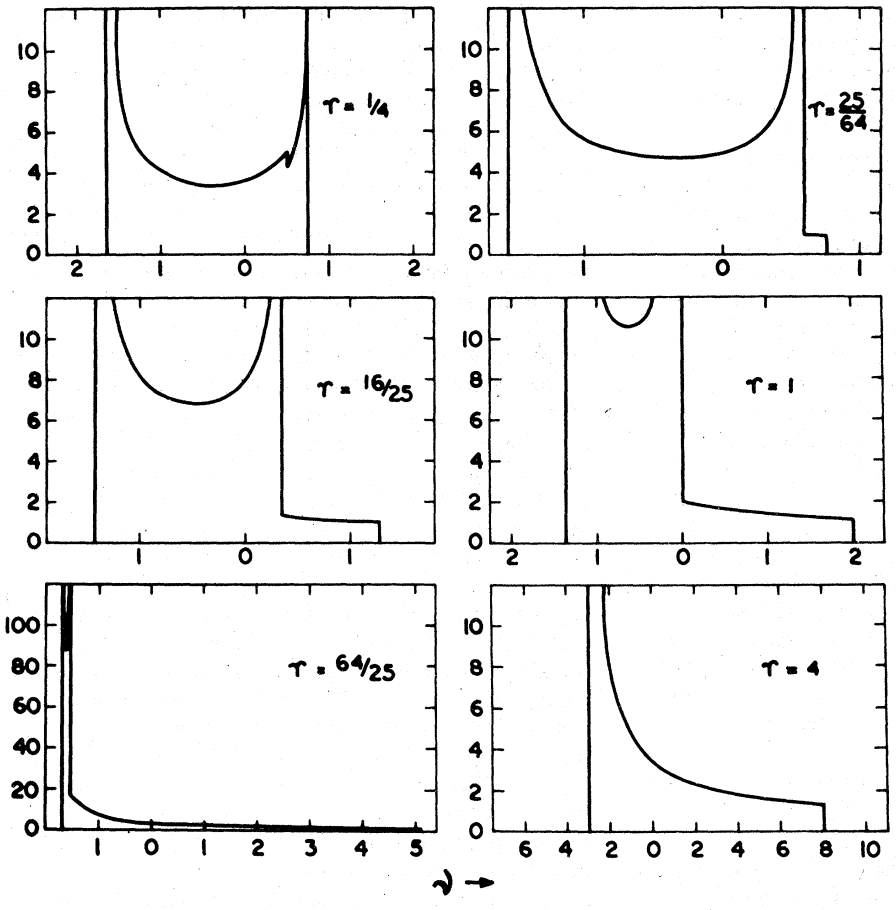

FIG. 2. Line-shape functions calculated by Jones *et al.*[21] for different r values ($r>0$).

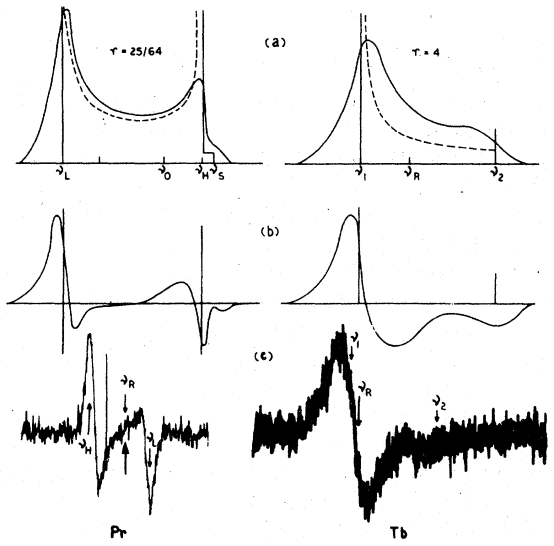

FIG. 3. NMR powder pattern for the central transitions with two widely different r values: (a) calculated absorption (--- in absence of dipolar broadening), (b) calculated absorption derivative, (c) experimental ^{51}V NMR spectra in $PrVO_4$ and $TbVO_4$

with frequency.

Frequency variation of ^{51}V NMR across the rare-earth series in RVO_4 exhibited various kinds of line shapes depending on r. It may be pointed out that for the same value of r, different rare earths often exhibited differences in the line shape. This has been attributed to the differences in the intrinsic broadening of the line. The departure of the line shape from calculated frequency distribution becomes greater when the intrinsic width is larger. This will be discussed later, particularly for ^{51}V spectra of $GdVO_4$.

On the basis of the ^{51}V line shape, the RVO_4 system may be divided into two classes: (i) the first-half members ($f^n, n<7$), which always exhibit a split central transition in the frequency range 2–12 MHz and (ii) the second-half members ($f^n, n \geq 7$), which exhibit a single asymmetric line at high frequencies, which, however, splits at low frequencies.

The first-half members exhibit a second-order quadrupolar split pattern even at the highest available frequency value. The calculated line shape (Pr) (Figs. 2 and 3) of Jones *et al.*[21] for $r=\frac{25}{64}$ almost

simulate the spectra at 12 MHz. This indicates that magnetic-shift interaction is smaller than the quadrupolar one for the first half even at 12 MHz. A typical frequency-variation spectrum is shown in Fig. 4. As the frequency is lowered, the line shape remains basically the same as is expected for a second-order quadrupolar split line. However, the splitting between the two peaks increases. Thus the splitting varies inversely as ν_R for the first-half members of the series throughout the frequency range studied.

Spectra for the second-half members at 12 MHz exhibit a single asymmetric line, indicating the predominance of magnetic-shift interaction over the quadrupolar coupling at this particular resonance frequency. However, there are some subtle differences in the powder pattern among the individual members. Thus from Tb to Er a weak hump appears on the low-field side in the absorption derivatives. It may be pointed out that a similar line shape with a rather prominent hump has been obtained for the $R\mathrm{PO}_4$ system in which an axially symmetric magnetic interaction alone is present. Thus it may appear that in the $R\mathrm{VO}_4$ system, magnetic-shift interaction for Tb to Er is strong in comparison to that in Gd, Tm, and Yb, where the hump in the derivative spectra did not appear. As the frequency is lowered, the magnetic-shift interaction decreases and the hump that appeared in the spectra at 12 MHz could not be detected though the low-field wing is always wider. In case of Yb, however, the pattern is no longer a single line at 8 MHz. It gives a split central transition characteristic of second-order quadrupolar interaction, indicating that the ratio of the magnetic to quadrupolar interaction is least for Yb in this group. This is in conformity with the magnitude of the magnetic moment of Yb, which is smallest among the second-half members. As the frequency is further lowered (~6 MHz), the line splits for all members except Gd. Finally the splitting of the central transition for the second half varies approximately as the inverse of the resonance frequency (Fig. 4) in the frequency range 2–6 MHz only.

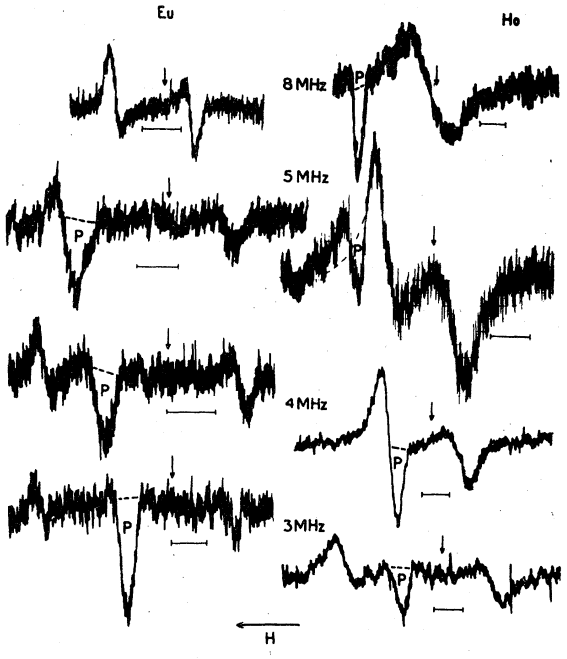

FIG. 4. ^{51}V NMR powder pattern (central transition) in EuVO_4 and HoVO_4 at different frequencies. --- indicates the mean ^{51}V line shape in absence of the probe signal (P). Calibrations (horizontal error bars) are equal to 20 kHz. The arrow gives the reference position and the increasing direction of the magnetic field H is shown.

The spectra of the Gd compound are rather anomalous at first sight. It has already been pointed out that there was no line splitting for Gd at 6 MHz, from which one may conclude that the magnetic interaction is strongest for Gd among the second-half members. However, a close examination reveals that this is not so. It is well known that among the rare earths, the half-filled shell ion Gd^{3+} is unique in having a rather long relaxation time and consequently a very large broadening of ^{51}V NMR line. This feature has complicated the NMR powder pattern of GdVO_4 (Fig. 5). Thus at 12 MHz, the line broadening has masked the hump observed in Tb, Dy, Ho, and Er. At 6 MHz also the line broadening possibly has affected the line splitting. Below this frequency range, however, there are definite indications of line splitting. Thus though the spectra at 4 and 2 MHz do not exhibit a sharp peak on the low-field side, the high-field peak is very prominent and satisfies the criterion of second-order quadrupolar splitting, viz., the shift of ν_L increases as $1/\nu_R$. The low-field peak is obviously smoothed out by the broadening. Thus the frequency-variation study of the central transition indicates that the magnetic interaction for the second half of the members of the $R\mathrm{VO}_4$ system is in the following order:

$$a_{\mathrm{Gd}} \simeq a_{\mathrm{Tb,Dy,Ho,Er}} > a_{\mathrm{Tm}} > a_{\mathrm{Yb}}.$$

The line-shape results uphold the analytical division of the rare earths into two groups. Thus the line shape in the first half is determined by second-order quadrupolar effect throughout the frequency range studied, whereas in the second half it is dominated by the magnetic interaction in the high-frequency range and the quadrupolar interaction is revealed only in the low-frequency range.

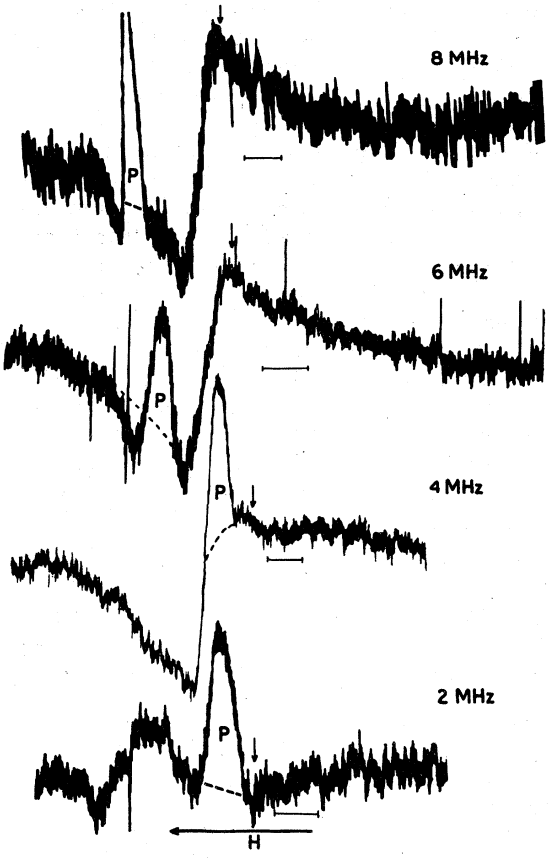

FIG. 5. ^{51}V NMR powder pattern (central transition) in $GdVO_4$ at different frequencies. All symbols are the same as in Fig. 4.

C. Estimation of K_{iso}, K_{an}, and ν_Q values

It has been shown that the rare-earth vanadates exhibit second-order quadrupolar splitting. Experimentally, the shifts of the ν_H and ν_L peaks of the split central transition were measured from the diamagnetic reference ν_R and were fitted to the expression given by Eqs. (10) and (11). The results are presented in Table I. As pointed out before, the broadening did not allow a well-defined split pattern for Gd, and therefore shifts could not be measured. Interestingly, Table I shows that though the sign of the anisotropic-shift interaction K_{an} is positive throughout the RVO_4 series, the sign of the isotropic shift K_{iso} changes. Further, the shifts for the second-half members are always an order of magnitude greater than those of the first half. Again, it may be pointed out that K_{an} is greater than K_{iso} throughout the series. All of these features are similar to ^{31}P in RPO_4.[9] Finally, the strengths of the quadrupolar interaction ν_Q as obtained both from the K_H and K_L plots agree fairly well with each other and are in the range 300–400 kHz. Table I contains the estimated r values for the different members at 12 MHz. Thus it falls into two different ranges, viz., $r \sim 0.50$ for the first-half members and $r \sim 2.0$ for the second-half members of the rare-earth series. Thus the second-order quadrupolar split spectra (Fig. 4) for the first-half members are consistent with the small r values, whereas the asymmetric single line for the second half is a reflection of the strong magnetic interaction as evidenced from the large r values.

TABLE I. Quadrupolar and magnetic-interaction parameters [a] of ^{51}V in the RVO_4 system.

	ν_Q (MHz)[b] from $\frac{1}{2} \leftrightarrow -\frac{1}{2}$		Shift[c] from K_H (%), K_L (%) vs ν_R^{-2} plot		r at
R^{3+}	K_H vs ν_R^{-2}	K_L vs ν_R^{-2}	K_{iso} (%)	a (%)	12 MHz
Ce	0.381	0.371	−0.020	0.030	0.3
Pr	0.381	0.378	−0.030	0.048	0.5
Nd	0.369	0.366	−0.025	0.075	0.8
Sm	0.370	0.363	−0.010	0.010	0.1
Eu	0.346	0.356	+0.020	0.045	0.6
Tb	0.336	0.327	+0.130	0.180	2.4
Dy	0.334	0.325	+0.100	0.200	2.7
Ho	0.330	0.330	+0.090	0.150	2.1
Er	0.324	0.318	+0.050	0.150	2.1
Tm	0.306	0.311	+0.045	0.110	1.8
Yb	0.300	0.307	+0.040	0.090	1.5

[a] Maximum uncertainties as estimated from the locations of the spectral features over the frequency range are ± 0.005 MHz in ν_Q values and ± 0.025% in K_{iso} and a values. Though K_{iso} values for some members of the first-half rare earths are within experimental uncertainty, repeated measurements indicated that the most probable K_{iso} values of the members from Ce to Sm are of negative sign, whereas that for Eu is of opposite sign.

[b] These ν_Q values agree with those obtained from single crystals in the case of some of the members (Ref. 8 and private communication by Prof. B. Bleaney).

[c] High- and low-field shifts are designated as negative and positive shifts, respectively.

V. DISCUSSION

A. Isotropic shift

It is well known that the shift of the ligand nuclei in rare-earth intermetallics and insulators changes sign[15,33] once across the series, upholding the $A_s\vec{I}\cdot\vec{S}$ form[12] of the hyperfine interaction (contact part). Further, alternation of the signs of the isotropic shift due to dipolar interaction (pseudo-contact) has also been observed in solution several times, across the series, in agreement with the theoretical prediction.[34] In the case of ^{51}V NMR in rare-earth vanadates, the sign reversal of the shift occurs only once at Eu (Fig. 6), indicating

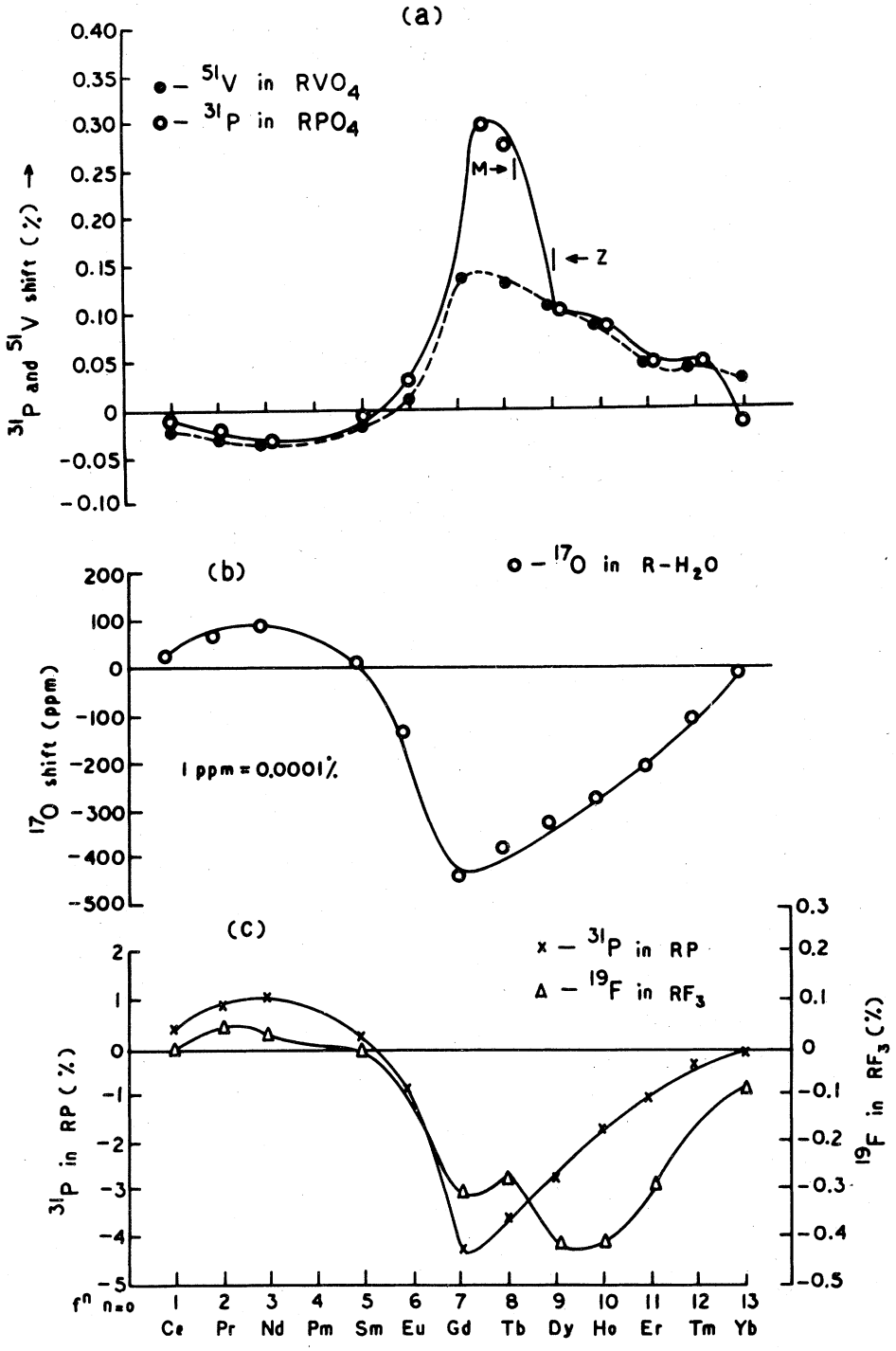

FIG. 6. Sign reversal of NMR shifts of the ligand nuclei across the rare-earth series in various compounds: (a) next-nearest neighbors in solid state, (b) nearest neighbors in solution, (c) nearest neighbors in solid state.

the contact nature of the shift, as observed in other systems. The sign reversal, though originally observed[33] and expected to occur always at Gd, in many systems,[9,15,35] including the present one, actually occurs at Eu because of the appreciable contribution of the excited state to the ground state of the Eu^{3+} ion. To have an idea about the quantitative aspect of the contact interaction across the series, one can utilize the relation[36] for the contact shift

$$K = A_S \langle S_z \rangle / g_N \mu_N , \tag{12}$$

where g_N and μ_N are the nuclear gyromagnetic ratio and the nuclear magneton, respectively, $\langle S_z \rangle$ is the average z component of the rare-earth spin, and A_s is the coupling constant. $\langle S_z \rangle$ values calculated by Golding and Halton explain the sign reversal at Eu. The plot (Fig. 7) of the experimental ^{51}V shift against the calculated $\langle S_z \rangle$ values of the rare earth ions is basically linear. However, the small departure indicated by arrows from linearity may be attributed to the small dipolar (pseudocontact) and local-field interaction. The linear plot indicates that the contact interaction is the dominant one in spite of ^{51}V being not directly bonded to the rare earth.

As stated earlier, the shift for the Gd compound could not be estimated from the frequency variation of the powder pattern. This linear plot facilitates getting the value for Gd (obtained by extrapolation). Thus the shift in $GdVO_4$ is found to be ~0.12%. Further, the slope of this line furnishes the average value (0.68 kOe) of the hyperfine field $H^{hf}(=A_s/\gamma\hbar)$ for the isostructural series. The hyperfine field per unit spin for individual members may also be obtained from the contact shift by using the relation[12]

$$H^{hf} = [N g_J \mu_B / (g_J - 1)\chi_M] K_{iso} , \tag{13}$$

where g_J is the Landé g factor for the rare-earth ion in question, N is the Avogadro number, and χ_M the molar susceptibility. Equation (13) has been utilized to estimate H^{hf} from K_{iso} and χ_M at a particular temperature. The susceptibility of these compounds has been found to be very close to ionic values. As χ_M data for the whole set of RVO_4 are not available, the ionic susceptibilities have been used in Eq. (13). It may be mentioned that Eq. (13) is not valid[12] for Sm^{3+} and Eu^{3+} compounds, since $\langle S \rangle \neq (g_J - 1)\langle J \rangle$ at room temperature for these two ions. These hyperfine-field values agree in order of magnitude with those calculated from Fig. (7).

Further, to obtain an idea of the covalent admixture, the fractional unpairing f_s of the vanadium 4s electron has been calculated from the relation[37]

$$f_s = (2S/N')(A_s/A_{4s}). \tag{14}$$

The f_s values presented in Table II are rather small in comparison to the value obtained[32] in the case of $LiCuVO_4$, corroborating the predominantly ionic nature of the rare-earth–vanadate bond.

As 4f electrons in rare-earth ions are well shielded by outer electrons (5s, 5p), participation of the 4f electrons in the bond is of less importance. The observed[15] magnitude and sign of the ^{17}O shifts point to the fact that a weak bond is formed between oxygen 2s and rare-earth 6s electrons. Examination of the consequence of direct 4f participation in the bond rules out any significant 4f contribution.[36] Direct 4f participation in GdF_3 has also been shown[38] to be very small. Recently, however, Mustafa *et al.*[39] interpreted ^{19}F shifts in ErF_3 in terms of f-electron participation

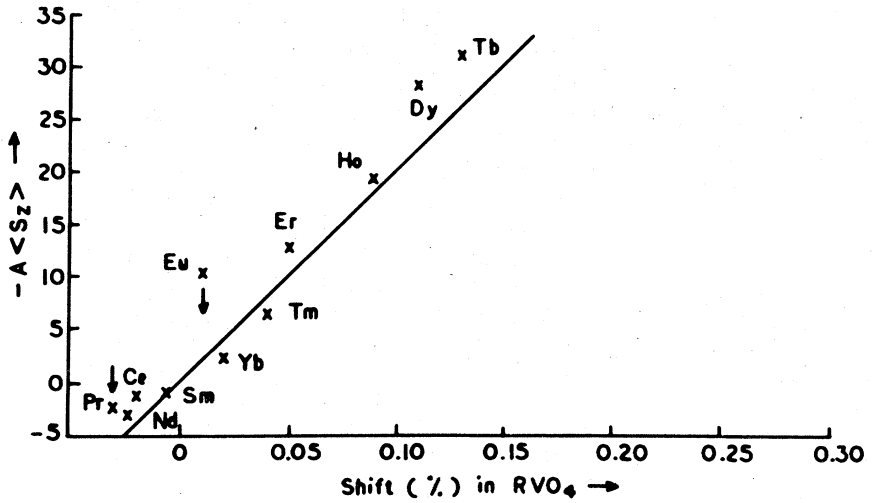

FIG. 7. Plot of $-A\langle S_z \rangle$ values (Ref. 36) ($A = 3kT/\mu_B H$) of rare-earth ions against the isotropic shifts in RVO_4 systems.

TABLE II. ^{51}V Hyperfine field, the hyperfine constant, and the fractional unpairing in rare-earth vanadates.[a]

R^{3+}	H^{hf} (kOe)	A_s[b] (10^{-5} cm^{-1})	f_s[c] (%)
Ce	2.58	9.62	0.0098
Pr	1.26	4.70	0.0092
Nd	0.69	2.57	0.0075
Sm	•••	•••	•••
Eu	•••	•••	•••
Gd	0.50	1.86	0.0128
Tb	0.60	2.26	0.0133
Dy	0.52	1.96	0.0096
Ho	0.55	2.05	0.0080
Er	0.44	1.66	0.0049
Tm	0.72	2.70	0.0052
Yb	2.13	7.94	0.0077

[a] The uncertainties in H^{hf}, A_s, and f_s values are determined primarily by the uncertainties in K_{iso} values given in Table I.

[b] A_{4s} (^{51}V) = 0.170 cm^{-1} [Saji (Ref. 33)].

[c] f_s was calculated using Eq. (14) with $N' = 6$.

and exchange polarization simultaneously. Results on vanadates, as also on phosphates,[9] however, suggest the charge transfer or exchange-polarization mechanism to be of importance.

As has been mentioned earlier, though data on the transferred hyperfine effect of the ligand nuclei directly attached to the rare-earth ion are available, work on the second-nearest neighbor is really meager. The result on the oxysalts presented here fills the gap partially and upholds a distinct feature of the spin transfer from the first to the second neighbor. In the 3*d* transition series, shifts exhibited by nuclei attached to the 3*d* ion either directly[40] or through an intervening oxygen[32,41] atom are of the same sign. Thus in the 3*d* system a parallel spin is transferred both to the first- and the second-nearest neighbors, whereas in the 4*f* system the spin transferred to the first neighbor is antiparallel and that at the next-nearest neighbor is parallel to the 4*f* spin. As such, the mechanism of spin transfer within the XO_4 group seems to be different in 3*d* and 4*f* systems.

B. Anisotropic shift

The experimental ^{51}V anisotropic shifts are positive for all the members of the series, unlike the isotropic shifts that exhibit a sign reversal across the series. The anisotropic shift primarily consists of two (the hyperfine and the dipolar) parts. They may be represented[9,14,18-20] by

$$K_{an}^{dip} = \alpha(3\cos^2\theta - 1)\chi_M, \tag{15}$$

$$K_{an}^{hf} = A_p(3\cos^2\theta - 1)\langle S_z\rangle, \tag{16}$$

where α is a constant characteristic of the crystal lattice.

The variation of the observed anisotropic shift and the susceptibility of the rare-earth ions along the rare-earth series are plotted in Fig. 8. The figure shows that the anisotropic shift has a trend similar to that of the susceptibility. It is interesting to note that for the given units of the shifts and the susceptibilities, a situation is obtained where the shift curve lies above the susceptibility curve for the first-half members, whereas it falls below the same curve for most of the second-half members. This may be explained as follows. For the first-half members, both the dipole and the hyperfine contribution act in the same direction and the total shift exceeds the dipolar part, whereas for the second half the hyperfine shift changes sign [according to Eq. (16)] and acts in opposition to the dipolar part, causing the resultant shift to fall below the level of the dipolar shift. This indicates the predominance of the dipolar effect in relation to the hyperfine one. An attempt has been made to separate the K_{an}^{hf}.

If one assumes that the structural parameters as well as the hyperfine-interaction constant remain more or less the same across the series, it is possible to estimate the K_{an}^{hf} and K_{an}^{dip} contributions. Using the values of the ionic susceptibilities and the calculated $\langle S_z\rangle$ of the rare earths, the experimental anisotropic shifts for any two members of the RVO_4 series may be fitted to the equation

$$K_{an} = A_1\langle S_z\rangle + A_2\chi_M, \tag{17}$$

and the constants A_1 and A_2 can be estimated. $A_1\langle S_z\rangle$ values obtained from such a calculation are roughly five times less than those for $A_2\chi_M$. Multiplying A_1, which is positive in sign, with the corresponding $\langle S_z\rangle$ one may obtain K_{an}^{hf}. An order-of-magnitude calculation[32,37] of the fractional unpairing f_p of the vanadium 4*p* orbital suggests $f_p \sim 0.0001\%$ in the rare-earth vanadates. The separated K_{an}^{hf} exhibited a sign reversal across the series like K_{iso}. However, unlike the isotropic shift, K_{an}^{hf} for the first-half members is positive, while it is negative for the second-half members. This implies that the sign of the isotropic hyperfine constant A_s is opposite to that of the anisotropic hyperfine constant A_p in the vanadates. In the case of transition-metal complexes, viz. $LiCuVO_4$, it has also been found[32] that the ^{51}V isotropic-shift constant K_{iso} is of opposite sign to that of K_{an}. It may be mentioned that the NMR anisotropic shift (hyperfine) is sensitive to the difference in occupancy of the p_σ and p_π orbitals.[24] The small value of the hyperfine constant may be explained in terms of the cancellation of the p_σ bond-

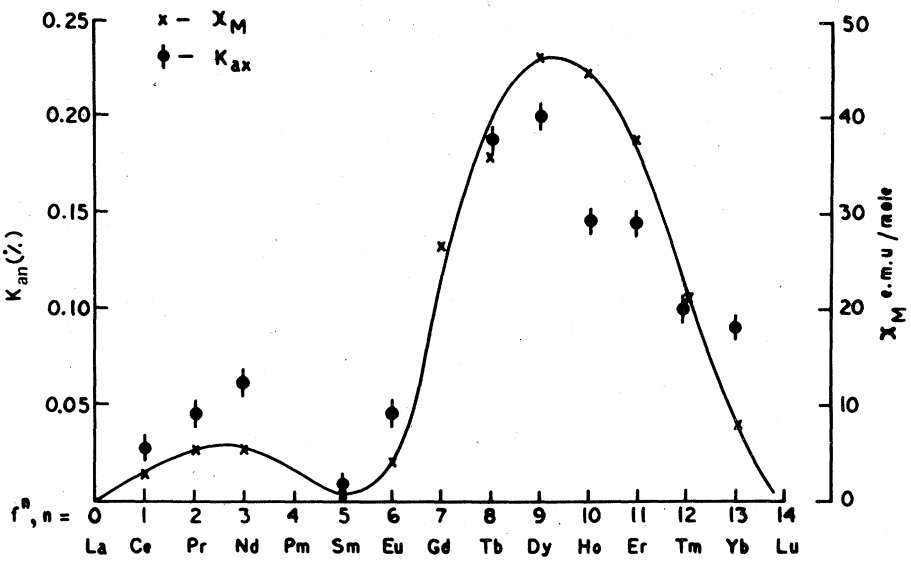

FIG. 8. ^{51}V anisotropic shifts K_{an} (obtained from a values in Table I) in the RVO_4 system as a function of f^n configuration. The variation of the ionic susceptibility χ_M across the series is also shown.

ing by a comparatively large amount of p_π bonding. The assumption that the anisotropic interaction is more or less constant may be justified by the similar outer-electron configuration of the rare-earth ions. This may be contrasted with the results on transition-metal compounds, where the d-electron configuration does not remain the same[42] for all the members. Thus, a large amount of p_σ bonding is observed in $KNiF_3$, whereas p_π bonding is large in K_2NaCrF_6.

C. Quadrupolar interaction

The electric field gradient at the site of a nucleus is known to depend[24] on the extent of covalent interaction and on the lattice parameters. In purely ionic crystals it is sufficient to treat all the ions as point charges for the calculation of the field gradient, whereas in covalent compounds a significant contribution to the field gradient from the bonding electrons of the non-s orbitals, must be taken into account.

The ^{51}V NMR in RVO_4 revealed the presence of quadrupolar interaction throughout the rare-earth series (Table I). It has also been found that the strength of the interaction significantly differs[11] in the two types of crystal structure of diamagnetic $LaVO_4$. In monoclinic $LaVO_4$, the quadrupolar interaction is of first order, while it is of second order in tetragonal $LaVO_4$. Thus the quadrupolar interaction in the more symmetric zircon form is greater than in the monoclinic structure with lower symmetry. The ^{51}V quadrupolar coupling in RVO_4 may now be compared (Table III) with other rare-earth systems, as there are some interesting features in the quadrupolar coupling constant of these systems. First, crystals having low lattice symmetry exhibit a smaller value of the quadrupolar coupling. Thus in RCl_3 the ^{35}Cl nuclear quadrupole resonance (NQR) frequency in the hexagonal structure is greater than in the monoclinic form. Second, the quadrupolar coupling of nuclei in these systems shows a slow variation along the series. However, it has been shown that the coupling constant in RVO_4, RAl_2, and RAl_3 decreases along the series, whereas it shows a systematic increase across the series in RCl_3 and $RAlO_3$.

It has been mentioned that the lattice constants and the extent of covalent interaction both determine the field gradient. In intermetallics of the type RAl_2, RCo_2 one finds a discrepancy[43] between the measured values of ^{27}Al and ^{59}Co coupling constants and those estimated from the ionic model. It has been commented by the authors that since the calculated ion-lattice contribution to the coupling constant exceeds the measured value in magnitude, the net contribution from other sources, e.g., conduction electrons and bonding electrons, must be opposite in sign to the ion-lattice contribution. In the case of proper rare-earth compounds, viz., RCl_3, the ^{35}Cl NQR frequencies increase smoothly in the series from $LaCl_3$ to $GdCl_3$ (hexagonal) by 27%, while the calculated electric-field gradient based on the point-charge summation model of de Wette and Schacher[46] increases only by 11% (Fig. 9). Similarly, the increase in the observed frequency versus atomic number for the monoclinic rare-earth chlorides (R = Tb–Yb) is less steep in calculations than in experiments. Again, the ^{27}Al quadrupolar coupling in $RAlO_3$,[17] an oxysalt, could not be accounted for by point-charge calculations. The failure of the point-

TABLE III. Quadrupolar-interaction parameters in various rare-earth systems.[a]

R^{3+}	$[e^2qQ/h]$ (MHz)				ν_Q (MHz)	Crystal parameters c/a in	
	^{51}V in RVO_4	^{27}Al in RAl_2	^{27}Al in RAl_3	^{27}Al in $RAlO_3$	^{35}Cl in RCl_3	RVO_4	RCl_3
	1	2	3	4	5	6	7
La	0.91±0.07 (*M*)						
La	5.92±0.07 (*T*)	3.97	•••	•••	4.167 (*H*)	0.8655	0.5845
Ce	5.33±0.07 (*T*)	4.72	•••	•••	4.387 (*H*)	0.8779	0.5789
Pr	5.23±0.07 (*T*)	4.60	•••	•••	4.566 (*H*)	0.8779	0.5759
Nd	5.18±0.07 (*T*)	4.56	•••	•••	4.729 (*H*)	0.8780	0.5731
Sm	5.08±0.07 (*T*)	•••	•••	•••	5.030 (*H*)	0.8799	0.5653
Eu	4.97±0.07 (*T*)	•••	•••	•••	•••	0.8798	0.5608
Gd	4.75±0.07 (*T*)	•••	•••	5.8533	5.315 (*H*)	0.8805	0.5573
Tb	4.68±0.07 (*T*)	•••	•••	5.9333	•••	0.8809	
Dy	4.57±0.07 (*T*)	•••	•••	8.6660	4.203 (*M*)	0.8837	
Ho	4.63±0.07 (*T*)	3.56	•••	•••	4.334 (*M*)	0.8835	
Er	4.48±0.07 (*T*)	3.45	8.3	•••	4.420 (*M*)	0.8842	
Tm	4.34±0.07 (*T*)	3.45	7.6	•••	•••	0.8857	
Yb	4.21±0.07 (*T*)	2.30	7.2	•••	4.730 (*M*)	0.8871	

[a]References: column 1, present work; column 2, Ref. 43; column 3, Ref. 31; column 4, Ref. 17; column 5, Ref. 44; column 6, Ref. 26; column 7, Ref. 45. *H*—hexagonal; *M*—monoclinic; *T*—tetragonal.

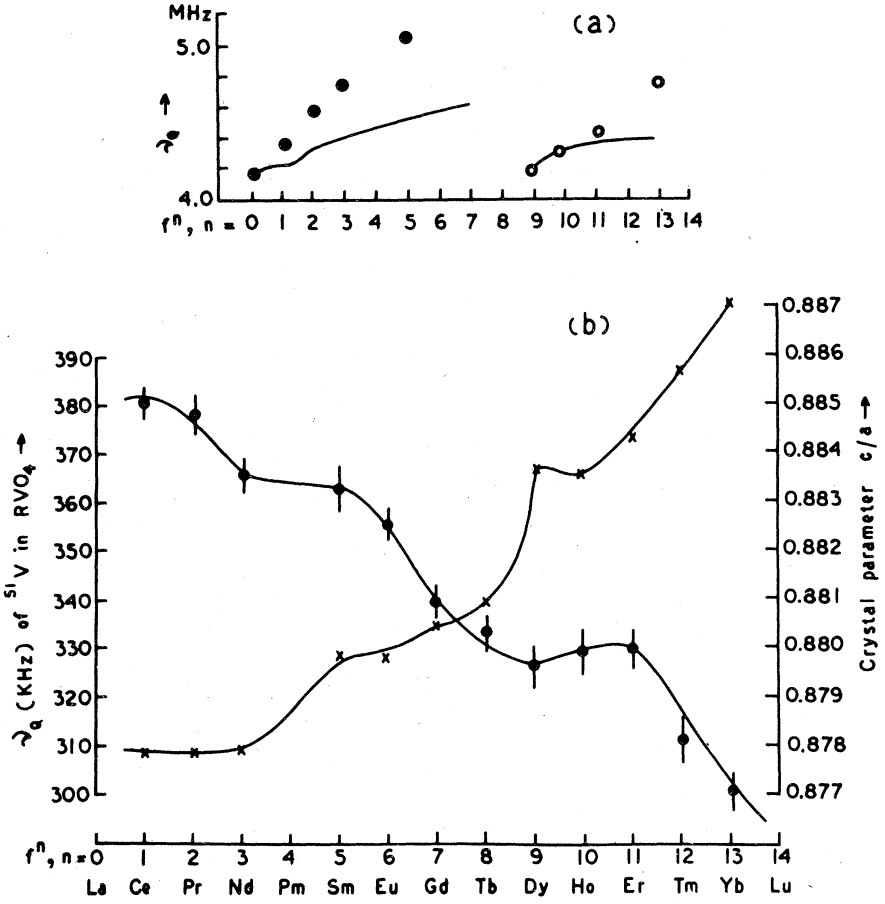

FIG. 9. Variation of the quadrupolar interaction parameter ν_Q across the rare-earth series. (a) ν_Q of ^{35}Cl in the hexagonal (●) and monoclinic (○) forms of RCl_3. —— calculated values. (b) ν_Q (●) of ^{51}V in RVO_4. The variation of the c/a ratio (×) is also shown.

charge model to predict correctly the frequency shifts in these series of isomorphic salts probably indicates the presence of a covalent interaction in these systems. The results on the magnetic hyperfine interaction in the vanadates indicated the presence of unpairing in the p orbital of the ligand nuclei. Thus the bonding electrons of non-s orbitals contribute to the field gradient at the vanadium site in vanadates. Further, the NMR in the oxysalts suggested that the magnetic interaction is greater[9] in the monoclinic form than in the zircon form.

Against this background, two observed features of the ^{51}V quadrupolar coupling in rare-earth vanadates will be discussed. One of the features is that the value of e^2qQ/h is less[11] in the monoclinic form, which seems to show stronger bonding effects as revealed in the studies of magnetic shifts.[9] The total field gradient may be represented as

$$q_{\text{tot}} = q_B(1-R) + q_L(1-\gamma_\infty), \tag{18}$$

where $(1-R)$ and $(1-\gamma_\infty)$ are the Sternheimer factors which correct for the polarization of the core by the electric field gradient of the valence and the lattice charge distribution, respectively, and the subscripts B and L indicate bonding and lattice contributions. In the case of predominantly ionic compounds, it is the q_L part that is expected to dominate over q_B. If q_B is assumed to act in opposition to q_L, q_{tot} will be less for a system where the bonding is comparatively large. Thus, the fact that e^2qQ/h for monoclinic $LaVO_4$ is less than that for the zircon variety is understandable qualitatively. By a similar argument, one can explain the smaller values of the ^{35}Cl quadrupolar coupling in the less symmetric monoclinic rare-earth chlorides as compared to the values obtained for the hexagonal structure.

The other feature that has been observed in the ^{51}V quadrupolar coupling is that e^2qQ/h decreases across the rare-earth series. This behavior seems to be anomalous because in the isostructural RVO_4 system the distance between the ligand and the metal ion decreases due to lanthanide contraction of the series. This, in turn, would cause an increase of both q_B and q_L. Though q_B opposes q_L, it is expected that the dominant q_L part will ultimately determine e^2qQ/h. As such, an increasing trend in the value of e^2qQ/h along the series is expected. However, the experimentally observed decreasing trend can be qualitatively understood from the following considerations. As one moves along the rare-earth series, two distinct effects are observed; they are the lanthanide contraction and the changes in the c/a ratio of the lattice. Due to the lanthanide contraction, q_L always increases along the series, but the c/a ratio may increase or decrease along the series. In the former situation, q_L decreases, whereas it increases in the latter case. If it is accepted that the change in c/a ratio controls the variation of e^2qQ/h, the decreasing values of ^{51}V coupling constants in RVO_4 can be easily understood. The plot of c/a and e^2qQ/h along the series is shown in Fig. 9. The trends of the two curves are quite similar. The value of e^2qQ/h changes by 25% after 13 members. With similar arguments, the 30% change in e^2qQ/h of ^{35}Cl in RCl_3 (hexagonal), for seven members, can be qualitatively understood. In rare-earth chlorides, the c/a ratio decreases. Here the lanthanide contraction and the c/a ratio act in the same direction to enhance the change in e^2qQ/h, in comparison to the vanadate system where these two effects are in opposition. Though the qualitative understanding of the change in e^2qQ/h along the series could be understood from the lattice interaction alone, a quantitative estimation of these values incorporating bonding effects is necessary to produce satisfactory results.

ACKNOWLEDGMENTS

The authors are grateful to Mrs. A. Basu for various suggestions and her excellent cooperation in matters of experiment. The sincere assistance of D. Roy in the preparation of the samples is highly appreciated.

[1] A. Gehring and K. A. Gehring, Rep. Prog. Phys. 38, 1 (1975).
[2] R. J. Elliott, R. T. Harley, W. Hays, and S. R. P. Smith, Proc. R. Soc. London, Ser. A 328, 217 (1972).
[3] S. Spooner, J. N. Lee, and H. W. Moos, Solid State Commun. 9, 1143 (1971).
[4] R. T. Harley, W. Hays, A. M. Perry, and S. R. P. Smith, Solid State Commun. 14, 521 (1974).
[5] L. Bonsall and R. L. Melcher, Phys. Rev. B 14, 1128 (1976).
[6] B. Bleaney, Physica (Utrecht) 69, 317 (1973).
[7] B. Bleaney, F. N. H. Robinson, and M. R. Wells, Proc. R. Soc. London, Ser. A 362, 179 (1978).
[8] B. Bleaney, F. N. H. Robinson, S. H. Smith, and M. R. Wells, J. Phys. C 10, L385 (1977).
[9] M. Bose, M. Bhattacharya, and S. Ganguli, Phys. Rev. B 19, 72 (1979).
[10] M. Bose and S. Ganguli, Phys. Lett. A 48, 357 (1974).
[11] M. Bose and S. Ganguli, J. Phys. Soc. Jpn. 42, 1781 (1977).
[12] E. D. Jones, Phys. Rev. 180, 455 (1969).
[13] V. Saraswati and R. Vijayaraghavan, J. Phys. Chem. Solids 28, 2111 (1967).
[14] S. P. Gabuda, A. G. Lindin, Yu, V. Gagarinskii, L. R.

Batsanova, and L. A. Khirpin, Zh. Eksp. Teor. Fiz. 51, 707 (1966) [Sov. Phys. JETP 24, 469 (1967)].
[15]W. B. Lewis, J. A. Jackson, J. F. Lemons, and H. Taube, J. Chem. Phys. 36, 694 (1962).
[16]B. R. McGarvey, J. Chem. Phys. 65, 1955, 1962 (1976); M. R. Mustafa, B. R. McGarvey, and E. Banks, J. Magn. Reson. 25, 341 (1977).
[17]D. T. Edmonds and G. P. Gill, J. Phys. C 4, 1426 (1971).
[18]F. Keffer, T. Oguchi, W. O'Sullivan, and J. Yamashita, Phys. Rev. 115, 1553 (1959).
[19]T. Tsang, J. Chem. Phys. 40, 729 (1964).
[20]R. E. Payne, R. A. Forman, and A. H. Kahn, J. Chem. Phys. 42, 3806 (1965).
[21]W. H. Jones, Jr., T. P. Graham, and R. G. Barnes, Phys. Rev. 132, 1898 (1963).
[22]M. P. Petrov and G. A. Smolenskii, Fiz. Tverd. Tela 7, 2156 (1965) [Sov. Phys. Solid State 7, 1735 (1966)].
[23]G. J. Genossar, M. Kutznietz, and N. Meerovici, Phys. Rev. B 1, 1958 (1970).
[24]J. Owen and J. H. N. Thornley, Rep. Prog. Phys. 29, 675 (1966).
[25]M. Bose and M. Bhattacharya, Phys. Rev. B 13, 4961 (1976).
[26]H. Schwarz, J. Anorg. Allengem. Chem. 323, 44 (1962).
[27]R. W. G. Wyckoff, *Crystal Structure*, 2nd ed. (Interscience, New York, 1965) Vol. 3, pp. 15, 33.
[28]H. Saji, T. Yamadaya, and M. Asanuma, J. Phys. Soc. Jpn. 28, 913 (1970).
[29]R. M. Pletnev, V. N. Lisson, A. A. Fotiev, and A. A. Fotiev, Sov. Phys. Solid State 16, 2397 (1975).
[30]J. F. Baugher, P. C. Taylor, T. Oja, and P. J. Bray, J. Chem. Phys. 50, 4914 (1969); S. L. Segel and R. B. Creel, Can. J. Phys. 48, 2673 (1970).
[31]H. W. de Wijn, A. M. Van Diepen, and K. H. J. Buschow, Phys. Rev. B 1, 4203 (1970).
[32]H. Saji, J. Phys. Soc. Jpn. 33, 671 (1972).
[33]V. Jaccarino, B. T. Matthias, M. Peter, H. Suhl, and J. H. Wernick, Phys. Rev. Lett. 5, 251 (1960).
[34]B. Bleaney, J. Magn. Reson. 8, 91 (1972).
[35]M. Wittanowski, L. Stefaniak, H. Januszewsky, and Z. W. Wolkowski, Chem. Commun. 1573 (1971).
[36]R. M. Golding and M. P. Halton, Aust. J. Chem. 25, 2577 (1972).
[37]W. B. Lewis, W. B. Rabideau, M. H. Krikorian, and W. H. Wittemamam, Phys. Rev. 170, 455 (1968).
[38]R. E. Watson and A. J. Freeman, *Hyperfine Interactions*, edited by A. J. Freeman and R. B. Frankel (Academic, New York, 1967).
[39]M. R. Mustafa, W. E. Jones, B. R. McGarvey, M. Greenblatt, and E. Banks, J. Chem. Phys. 62, 2700 (1975); E. Banks, M. Greenblatt, and B. R. McGarvey, J. Chem. Phys. 58, 4787 (1973).
[40]E. D. Jones, Phys. Rev. 158, 295 (1967); R. G. Shulman and V. Jaccarino, Phys. Rev. 108, 1219 (1957).
[41]J. M. Mays, Phys. Rev. 131, 38 (1963).
[42]R. G. Shulman and K. Knox, Phys. Rev. Lett. 4, 603 (1960); R. G. Shulman and S. Sugano, Phys. Rev. 130, 506 (1963).
[43]R. G. Barnes and R. G. Lecandre, J. Phys. Soc. Jpn. 22, 1930 (1969); D. R. Torgenson and R. G. Barnes, Phys. Rev. 136, A734 (1964).
[44]E. H. Carlson and H. S. Adams, J. Chem. Phys. 51, 388 (1969).
[45]D. H. Templeton and C. H. Dauben, J. Am. Chem. Soc. 76, 5237 (1954).
[46]F. de Wette and G. Schacher, Phys. Rev. 137, A78, 92 (1965).